

Fig. S1. Variations of lattice parameters, unit-cell volume, and excess volume in the Ni-Co solid solution of the vivianite-type arsenates.

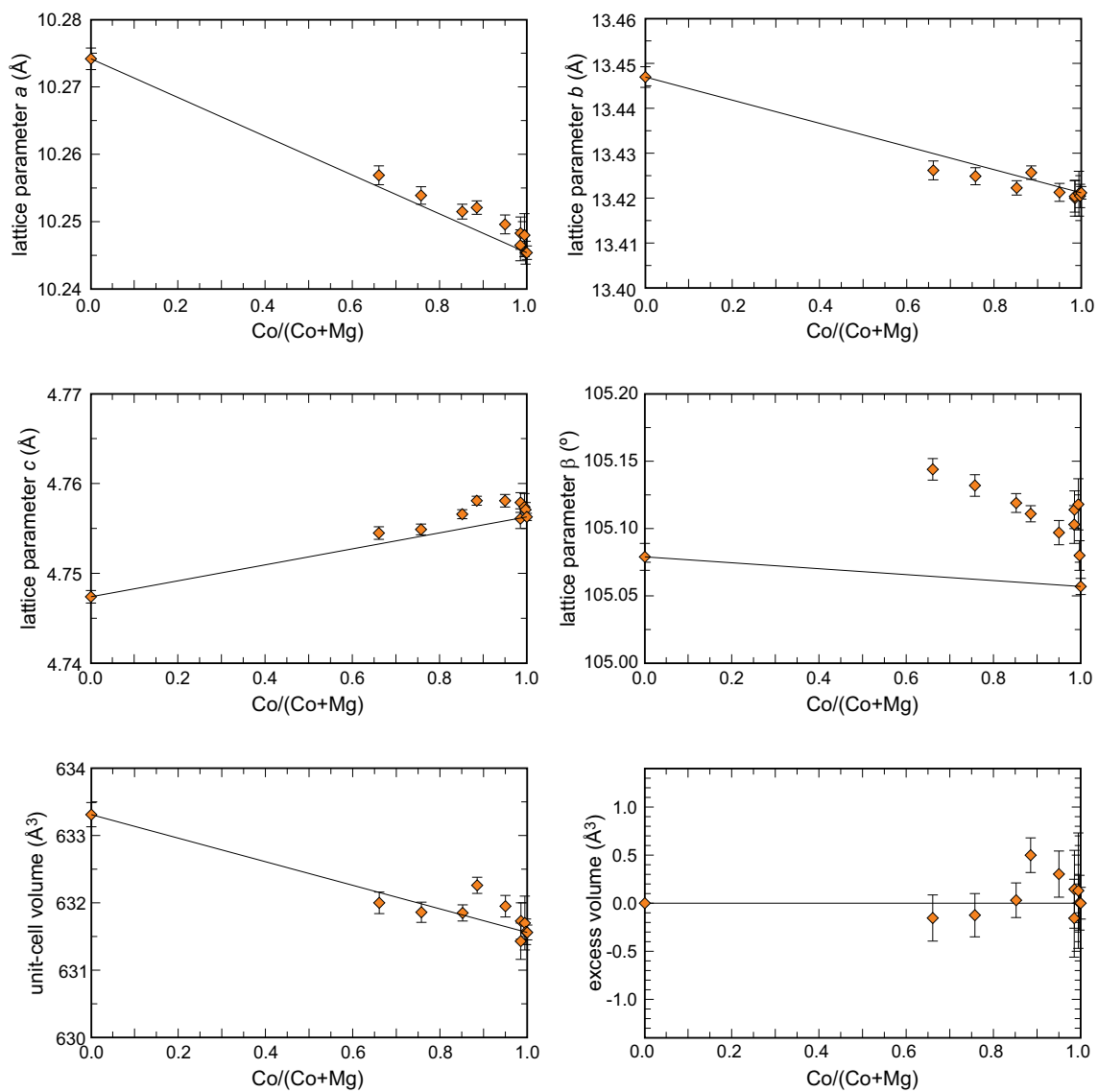


Fig. S2. Variations of lattice parameters, unit-cell volume, and excess volume in the Mg-Co solid solution of the vivianite-type arsenates.

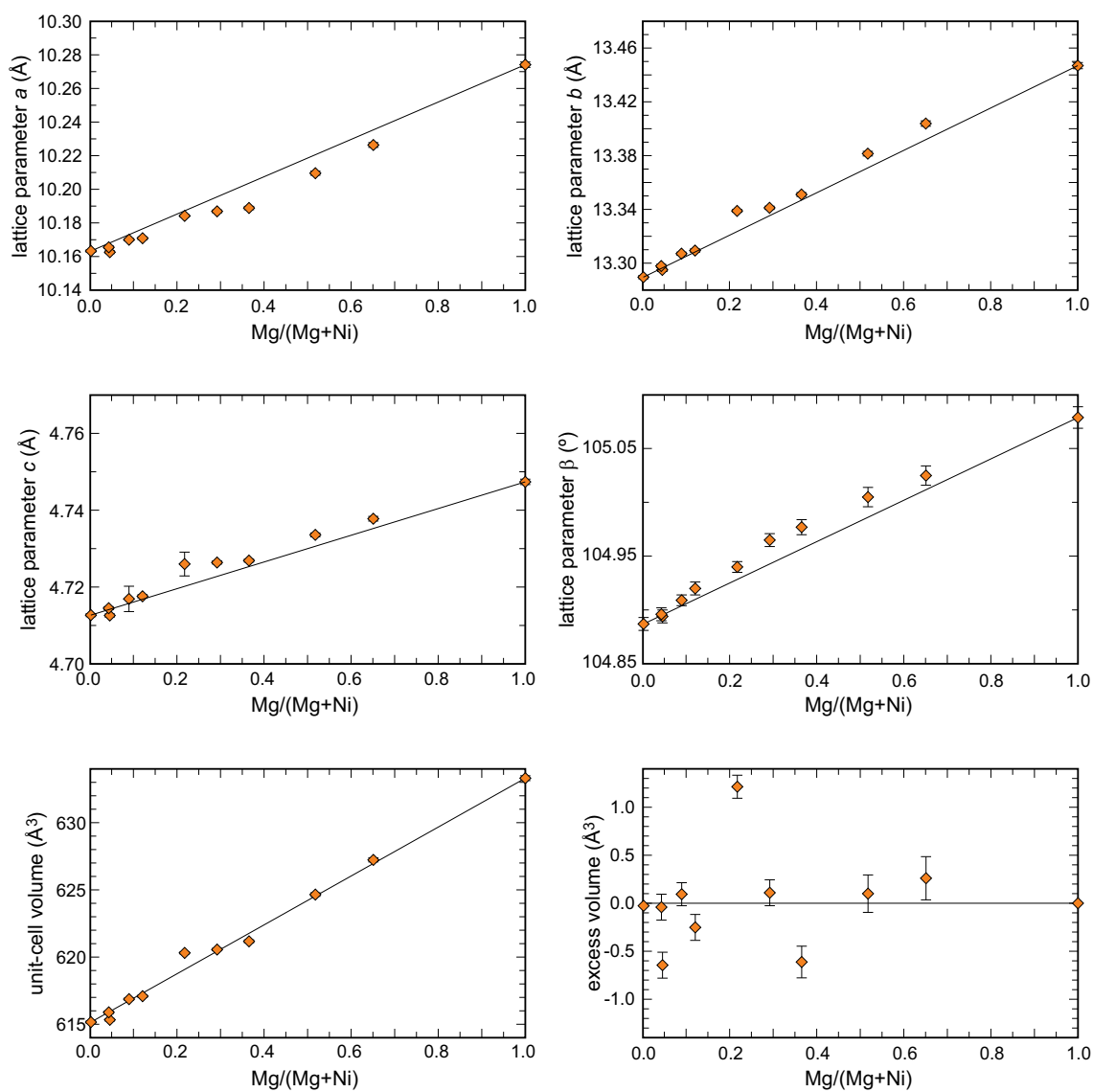


Fig. S3. Variations of lattice parameters, unit-cell volume, and excess volume in the Ni-Mg solid solution of the vivianite-type arsenates.

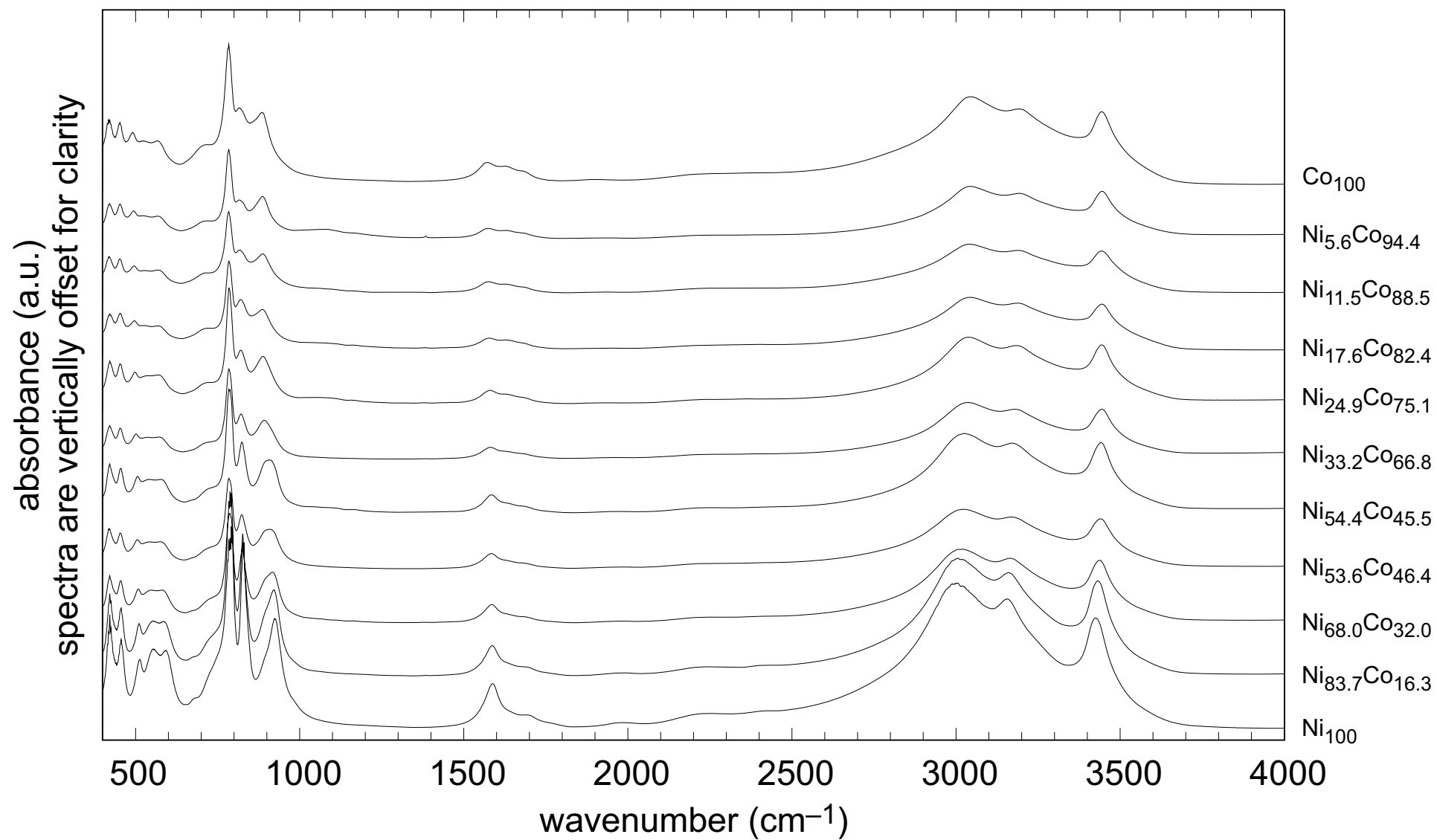


Fig. S4. Fourier-transform infrared (FTIR) spectra of the Ni-Co solid solution of the vivianite-type arsenates. The composition of the samples (in molar proportions of the cations) is indicated on the right-hand side of the diagram.

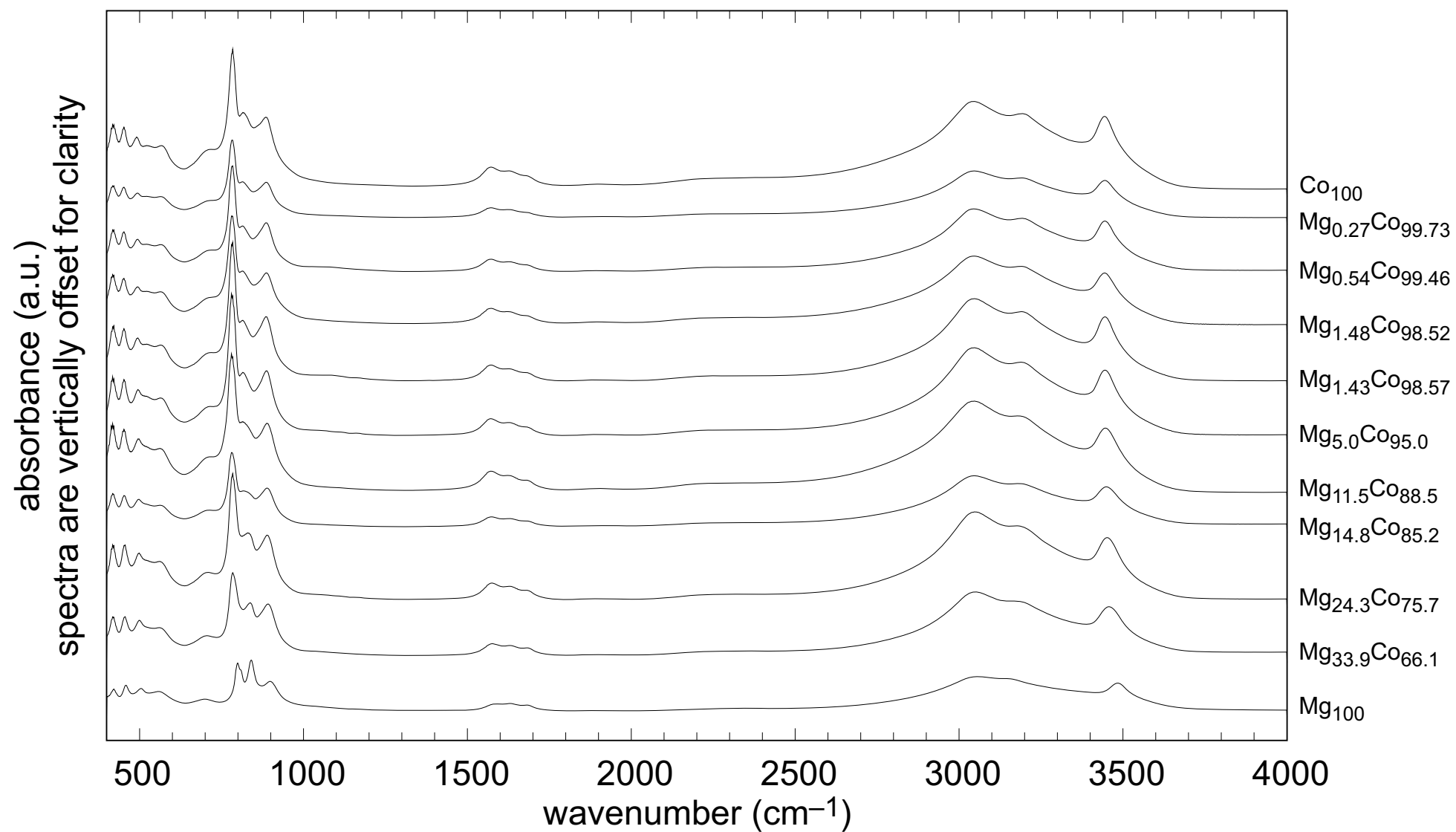


Fig. S5. Fourier-transform infrared (FTIR) spectra of the Mg-Co solid solution of the vivianite-type arsenates. The composition of the samples (in molar proportions of the cations) is indicated on the right-hand side of the diagram.

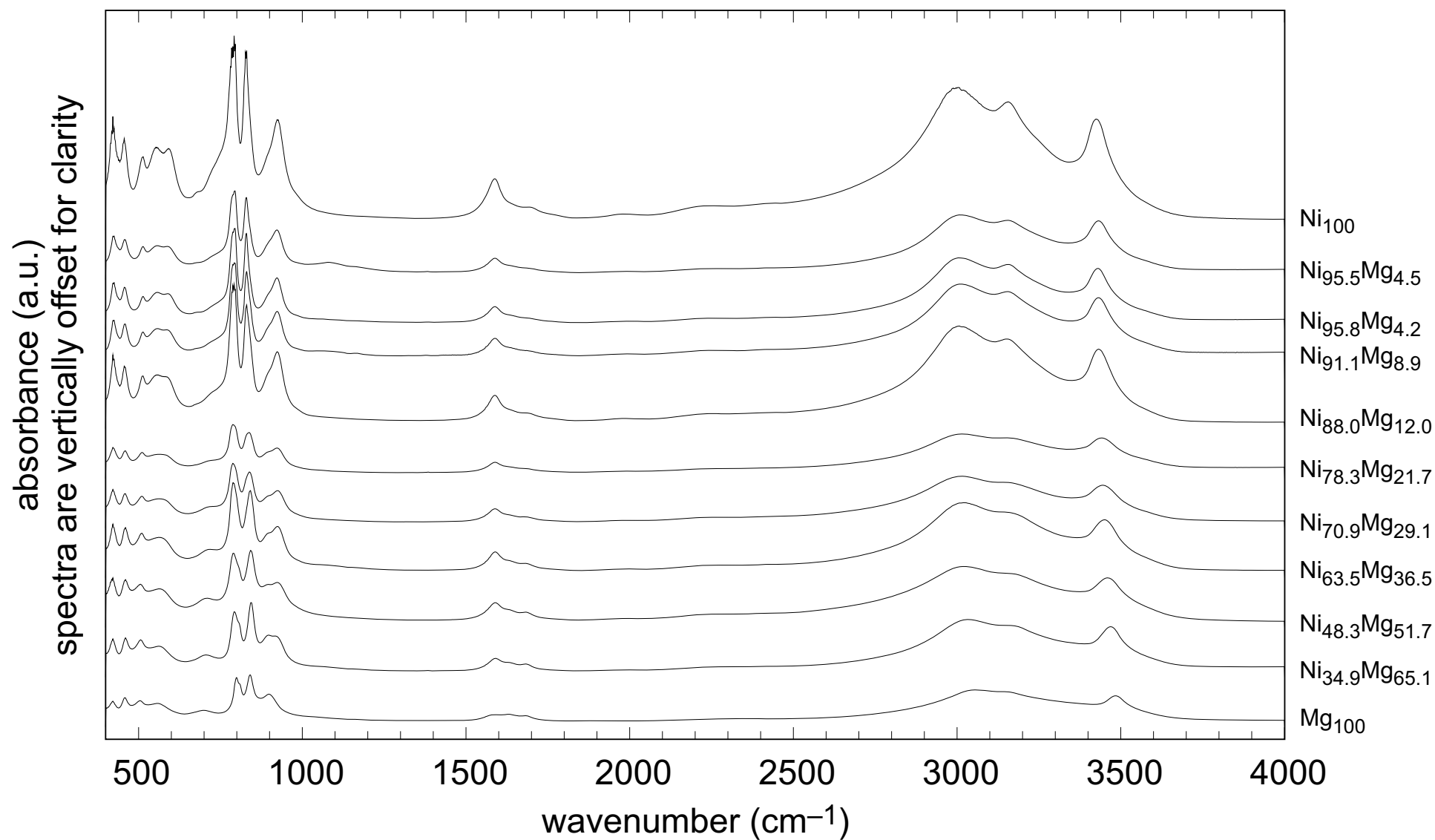


Fig. S6. Fourier-transform infrared (FTIR) spectra of the Ni-Mg solid solution of the vivianite-type arsenates. The composition of the samples (in molar proportions of the cations) is indicated on the right-hand side of the diagram.

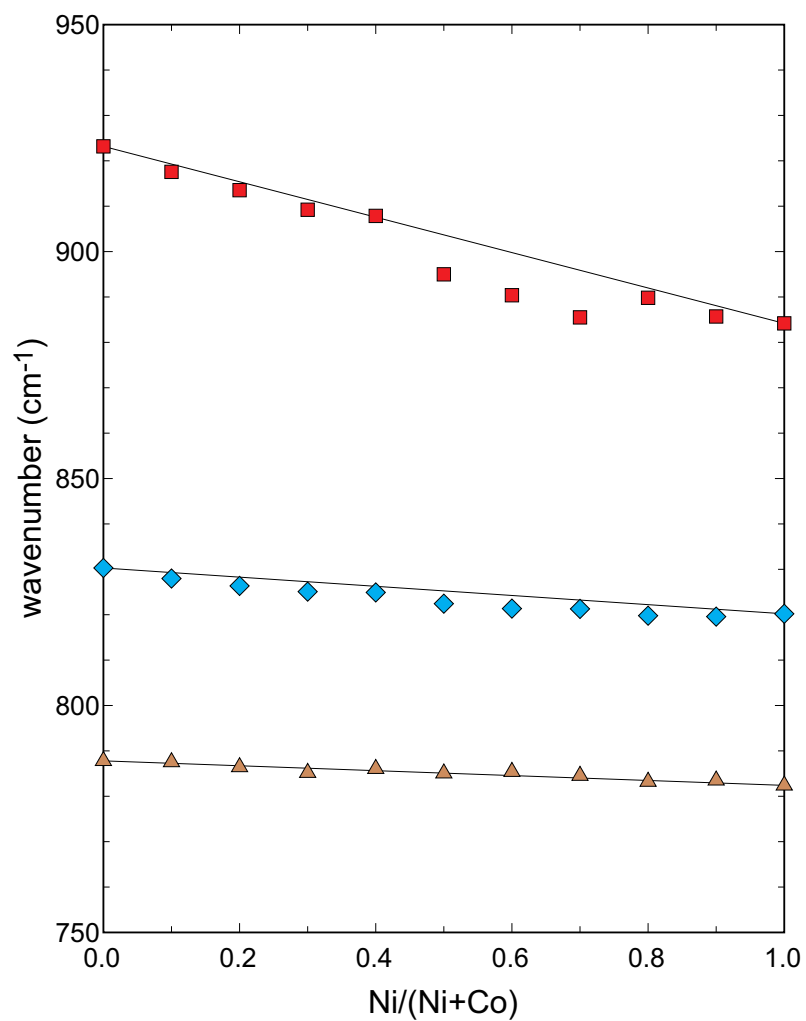


Fig. S7. Position of the arsenate vibrational bands (from the FTIR spectra) as a function of the molar Ni/(Ni+Co) ratio in the annabergite-erythrite solid solution.

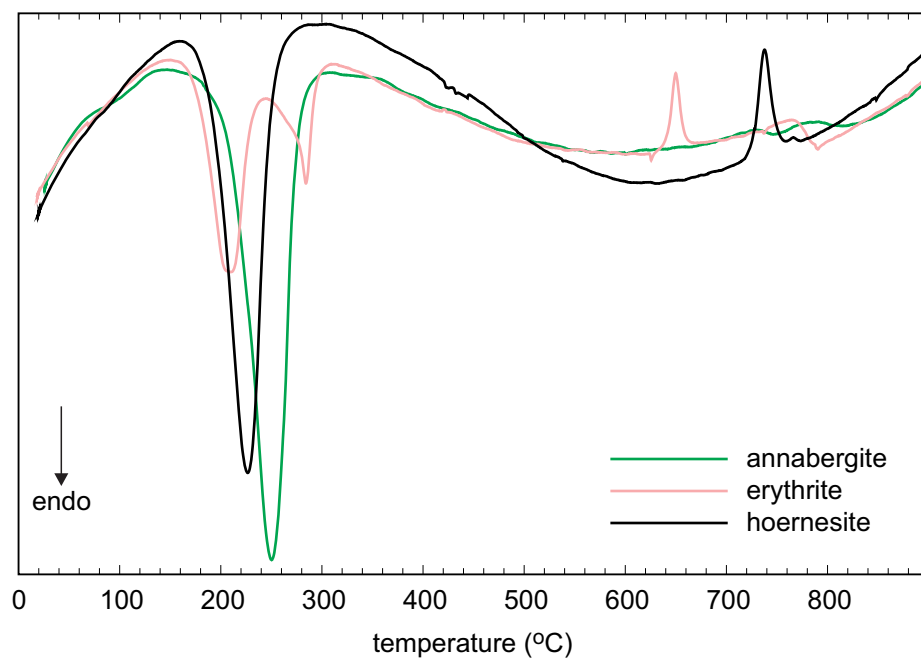


Fig. S8. Differential thermal analysis (DTA) data sets for the synthetic end members of the studied arsenates. A brief description of the data can be found in the text.

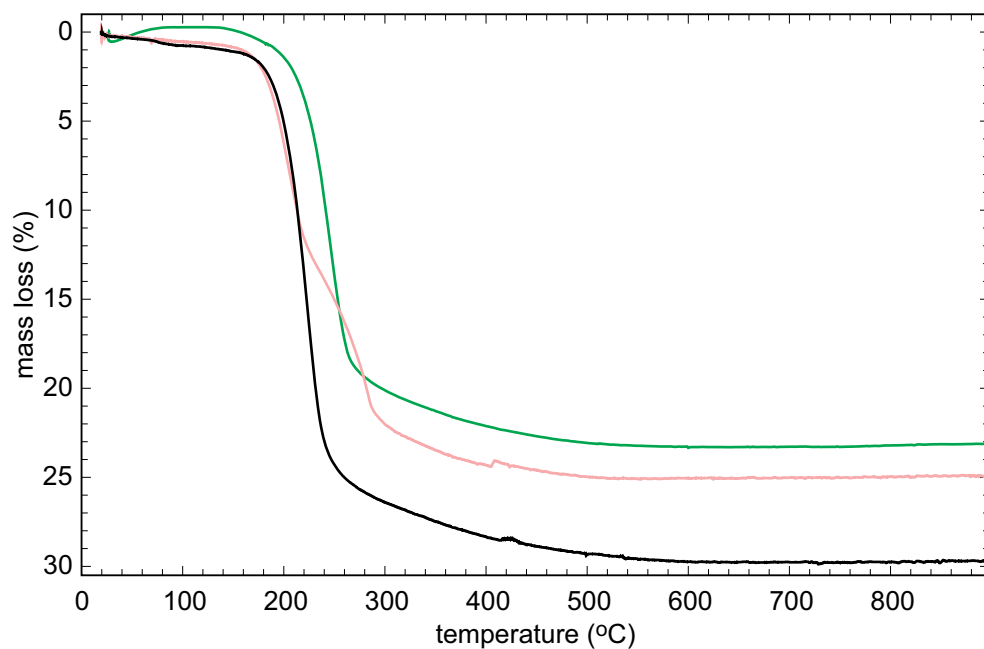


Fig. S9. Thermogravimetric (TG) data sets for the synthetic end members of the studied arsenates. A brief description of the data can be found in the text.